Ming Yueh Tan*, Karen A. Crouse, Sang Loon Tan and Edward R. T. Tiekink*

Crystal structure of bis{*N′*-[1,3-diphenylprop-2-en-1-ylidene]-*N*-phenylcarbamohydrazonothioato} zinc(II), $C_{44}H_{36}N_6S_2Zn$

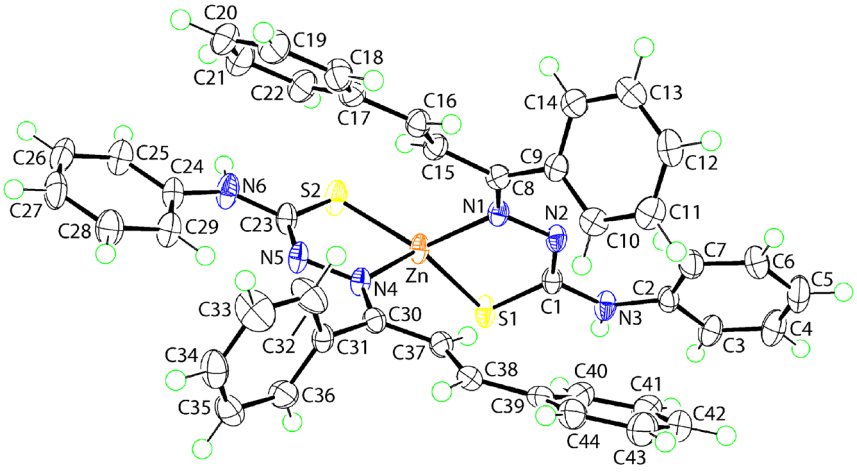

https://doi.org/10.1515/ncrs-2023-0369
Received August 11, 2023; accepted September 5, 2023;
published online October 10, 2023

Abstract

$C_{44}H_{36}N_6S_2Zn$, monoclinic, $P2_1/c$ (no. 14), a = 14.5676(4) Å, b = 26.1767(8) Å, c = 10.0963(3) Å, β = 99.140(3)°, V = 3801.2(2) Å^3, Z = 4, $R_{gt}(F)$ = 0.0397, $wR_{ref}(F^2)$ = 0.1000, T = 100 K.

CCDC no.: 1022760

The molecular structure is shown in the figure. Table 1 contains crystallographic data and Table 2 contains the list of the atoms including atomic coordinates and displacement parameters.

Table 1: Data collection and handling.

Crystal:	Yellow block
Size:	0.24 × 0.22 × 0.17 mm
Wavelength:	Mo *Kα* radiation (0.71073 Å)
μ:	0.80 mm^{-1}
Diffractometer, scan mode:	Oxford Diffraction Gemini, ω
θ_{max}, completeness:	25.2°, >99 %
$N(hkl)_{measured}$, $N(hkl)_{unique}$, R_{int}:	25,066, 8793, 0.038
Criterion for I_{obs}, $N(hkl)_{gt}$:	$I_{obs} > 2\ \sigma(I_{obs})$, 7212
$N(param)_{refined}$:	484
Programs:	CrysAlis^{PRO} [1], SHELX [2, 3], WinGX/ORTEP [4]

1 Source of material

4–Phenyl-3-thiosemicarbazide (Sigma Aldrich), trans-chalcone (Alfa Aesar), zinc acetate dihydrate (Fluka), concentrated hydrochloric acid (J. T. Baker), absolute ethanol (Merck), acetonitrile (Merck) and ethyl acetate (Merck) were of analytical grade and used as purchased. The Schiff base ligand was prepared from the 1:1 reaction of 4-phenyl-3-thiosemicarbazide (1.151 g, 0.01 mol) and trans-chalcone (2.083 g, 0.01 mol). Thus, the former was taken in heated absolute ethanol (30 mL) and slowly added to a heated ethanolic solution (20 mL) of the latter. A few drops of concentrated hydrochloric acid were added as a catalyst while stirring for 30 min. The yellow precipitate was filtered,

***Corresponding authors: Ming Yueh Tan,** Department of Physical Science, Faculty of Applied Sciences, Tunku Abdul Rahman University of Management and Technology, 50932 Setapak, Kuala Lumpur, Malaysia, E-mail: tanmy@tarc.edu.my; and **Edward R. T. Tiekink**, Research Centre for Crystalline Materials, School of Medical and Life Sciences, Sunway University, 47500 Bandar Sunway, Selangor Darul Ehsan, Malaysia, E-mail: edwardt@sunway.edu.my. https://orcid.org/0000-0003-1401-1520 (E.R.T. Tiekink)
Karen A. Crouse, Department of Chemistry, Faculty of Science, Universiti Putra Malaysia, 43400 UPM Serdang, Selangor Darul Ehsan, Malaysia
Sang Loon Tan, Research Centre for Crystalline Materials, School of Medical and Life Sciences, Sunway University, 47500 Bandar Sunway, Selangor Darul Ehsan, Malaysia

Table 2: Fractional atomic coordinates and isotropic or equivalent isotropic displacement parameters (Å^2).

Atom	*x*	*y*	*z*	U_{iso}*/U_{eq}
Zn	0.12384 (2)	0.55631 (2)	0.67161 (2)	0.01709 (7)
S1	0.07835 (4)	0.52445 (2)	0.86024 (5)	0.02072 (12)
S2	0.08557 (4)	0.63193 (2)	0.56935 (6)	0.02408 (13)
N1	0.10663 (11)	0.48340 (6)	0.59479 (16)	0.0161 (3)
N2	0.07628 (12)	0.44628 (6)	0.67626 (16)	0.0173 (4)
N3	0.02672 (13)	0.42932 (7)	0.87789 (17)	0.0196 (4)
H3N	0.0088 (16)	0.4431 (8)	0.9483 (16)	0.023*
N4	0.26020 (12)	0.57424 (6)	0.66131 (16)	0.0163 (3)
N5	0.27588 (12)	0.61819 (6)	0.59251 (17)	0.0189 (4)
N6	0.21043 (13)	0.68754 (7)	0.4743 (2)	0.0243 (4)
H6N	0.1577 (11)	0.7025 (9)	0.442 (2)	0.029*
C1	0.05962 (14)	0.46279 (8)	0.79200 (19)	0.0164 (4)
C2	0.01225 (14)	0.37621 (8)	0.8693 (2)	0.0183 (4)
C3	−0.02464 (15)	0.35358 (8)	0.9747 (2)	0.0226 (5)
H3	−0.039246	0.374119	1.046065	0.027*
C4	−0.03996 (17)	0.30152 (9)	0.9757 (2)	0.0293 (5)
H4	−0.065706	0.286630	1.047338	0.035*
C5	−0.01825 (17)	0.27075 (9)	0.8734 (3)	0.0309 (5)
H5	−0.028764	0.234949	0.874355	0.037*
C6	0.01895 (17)	0.29312 (9)	0.7700 (2)	0.0280(5)
H6	0.034771	0.272191	0.700080	0.034*
C7	0.03380 (16)	0.34545 (8)	0.7656 (2)	0.0231 (5)
H7	0.058406	0.360166	0.692668	0.028*
C8	0.13913 (13)	0.46721 (8)	0.48846 (19)	0.0165 (4)
C9	0.15347 (14)	0.41256 (8)	0.4579 (2)	0.0172 (4)
C10	0.20011 (14)	0.37977 (8)	0.5558 (2)	0.0199 (4)
H10	0.221547	0.392363	0.643519	0.024*
C11	0.21525 (16)	0.32910 (9)	0.5258 (2)	0.0244 (5)
H11	0.247595	0.307291	0.592626	0.029*
C12	0.18337 (16)	0.31009 (9)	0.3985 (2)	0.0249 (5)
H12	0.192489	0.275157	0.378706	0.030*
C13	0.13804 (15)	0.34243 (9)	0.3002 (2)	0.0235 (5)
H13	0.116824	0.329647	0.212650	0.028*
C14	0.12363 (14)	0.39329 (8)	0.3294 (2)	0.0201 (4)
H14	0.093184	0.415223	0.261221	0.024*
C15	0.16535 (14)	0.50709 (8)	0.40033 (19)	0.0183 (4)
H15	0.139644	0.540205	0.406358	0.022*
C16	0.22338 (14)	0.49986 (8)	0.3116 (2)	0.0190 (4)
H16	0.245596	0.466089	0.303033	0.023*
C17	0.25578 (14)	0.53903 (8)	0.22660 (19)	0.0188 (4)
C18	0.32258 (15)	0.52544 (9)	0.1477 (2)	0.0228 (5)
H18	0.345035	0.491325	0.149821	0.027*
C19	0.35648 (17)	0.56125 (9)	0.0661 (2)	0.0273 (5)
H19	0.401799	0.551567	0.012832	0.033*
C20	0.32414 (17)	0.61116 (9)	0.0625 (2)	0.0282 (5)
H20	0.347102	0.635638	0.006486	0.034*
C21	0.25851 (16)	0.62523 (9)	0.1405 (2)	0.0272 (5)
H21	0.236581	0.659443	0.138194	0.033*
C22	0.22448 (16)	0.58955 (9)	0.2221 (2)	0.0241 (5)
H22	0.179425	0.599594	0.275461	0.029*
C23	0.20083 (14)	0.64432 (8)	0.5474 (2)	0.0197 (4)
C24	0.28952 (15)	0.70936 (8)	0.4307 (2)	0.0216 (4)
C25	0.27369 (17)	0.75365 (8)	0.3530 (2)	0.0260 (5)
H25	0.212702	0.767420	0.333581	0.031*
C26	0.34610 (18)	0.77756 (9)	0.3043 (2)	0.0282 (5)
H26	0.334595	0.807636	0.251666	0.034*
C27	0.43498 (17)	0.75795 (9)	0.3319 (2)	0.0279 (5)
H27	0.484750	0.774285	0.298185	0.034*
C28	0.45084 (17)	0.71419 (9)	0.4091 (2)	0.0275 (5)
H28	0.512035	0.700677	0.428225	0.033*
C29	0.37911 (16)	0.68963 (9)	0.4593 (2)	0.0243 (5)
H29	0.391126	0.659728	0.512556	0.029*
C30	0.33492 (14)	0.54716 (8)	0.70240 (19)	0.0162 (4)
C31	0.42810 (14)	0.56527 (7)	0.6791 (2)	0.0162 (4)
C32	0.45855 (17)	0.55621 (9)	0.5577 (2)	0.0301 (5)
H32	0.421527	0.536434	0.490530	0.036*
C33	0.54277 (18)	0.57594 (11)	0.5341 (2)	0.0349 (6)
H33	0.563605	0.569197	0.451330	0.042*
C34	0.59678 (15)	0.60544 (9)	0.6306 (2)	0.0256 (5)
H34	0.654358	0.619026	0.614067	0.031*
C35	0.56645 (16)	0.61490 (9)	0.7503 (2)	0.0262 (5)
H35	0.603035	0.635311	0.816447	0.031*
C36	0.48253 (15)	0.59477 (9)	0.7753 (2)	0.0232 (5)
H36	0.462374	0.601267	0.858677	0.028*
C37	0.32229 (14)	0.49884 (8)	0.76695 (19)	0.0177 (4)
H37	0.262556	0.492158	0.789471	0.021*
C38	0.38743 (15)	0.46267 (8)	0.79781 (19)	0.0185 (4)
H38	0.448883	0.470343	0.783705	0.022*
C39	0.37050 (15)	0.41205 (8)	0.8519 (2)	0.0205 (4)
C40	0.29153 (16)	0.40097 (9)	0.9092 (2)	0.0266 (5)
H40	0.248872	0.427454	0.920479	0.032*
C41	0.27486 (18)	0.35160 (10)	0.9497 (2)	0.0347 (6)
H41	0.220100	0.344280	0.986206	0.042*
C42	0.3379 (2)	0.31302 (10)	0.9370 (2)	0.0370 (6)
H42	0.326581	0.279345	0.965490	0.044*
C43	0.4172 (2)	0.32339 (9)	0.8830 (2)	0.0342 (6)
H43	0.460827	0.296988	0.875282	0.041*
C44	0.43317 (17)	0.37255 (8)	0.8399 (2)	0.0260 (5)
H44	0.487442	0.379403	0.801698	0.031*

Table 2: (continued)

washed with cold ethanol and dried in vacuo. The zinc compound was prepared by the 1:2 reaction of zinc acetate dihydrate (0.220 g, 10 mmol) and the Schiff base (0.714 g, 20 mmol). Zinc acetate dihydrate was dissolved in heated ethanol (20 mL) and added to a solution of the Schiff base ligand in heated absolute ethanol (20 mL) while stirring for 30 min. The yellow precipitate was filtered, washed with cold ethanol and dried in vacuo. Single crystals were grown at room temperature from the slow evaporation of a mixture of acetonitrile and ethyl acetate (2:1 v/v). Yield: 70 %. Melting Point: 494–496 K. **FT–IR** (ATR (solid) cm^{-1}): 3411 ν(N–H), 1596 ν(C=N), 1314 ν(N–N), 487 ν(Zn–S), 533 ν(Zn–N). **UV–Visible** (nm; ε cm^{-1} mol^{-1} L): 246 (9.571×10^3), 292 nm (5.520×10^3), 400 (7.673×10^3). **ICP–AES**: Found % Zn = 8.03. Calc. % Zn = 7.53.

2 Experimental details

The C-bound H atoms were geometrically placed (C—H = 0.95 Å) and refined as riding with $U_{iso}(H) = 1.2U_{eq}(C)$. The N-bound H atoms were located in a difference Fourier map and refined with N—H = 0.88 ± 0.01 Å and with $U_{iso}(H) = 1.2U_{eq}(N)$. The maximum/minimum residual electron density peaks of 1.27 and 0.65 e Å^{-3} were located 0.87 and 0.66 Å, respectively, from the Zn atom.

3 Comment

Transition metal complexes derived from thiosemicarbazones, with generic formula $R^1N(R^2)C(=S)N(R^3)N=C(R^4)R^5$, where the substituents can be some combination of H/alkyl/aryl, continue to attract attention in, for example, nuclear medicine [5], as chemotherapeutic agents [6] and as catalysts [7]. The title complex (I) was investigated as a part of on-going studies into the generation and metal complexation by thiosemicarbazones derived from the condensation reaction between thiosemicarbazides and trans-chalcone, a flavonoid, and their saturated analogues [8, 9].

The molecular structure of (I) is shown in the figure (70 % displacement ellipsoids). The Zn atom is bis-chelated by the thiolato–S and imine–N atoms of two anions. The Zn—S1,S2 bond lengths are 2.2720(5) and 2.2611(6) Å, respectively, and the relatively long C—S1,S2 bonds [1.759(2) and 1.758(2) Å] substantiate the thiolato-character of the coordinated sulphur atoms. The Zn—N1,N4 bond lengths are 2.0603(17) and 2.0598(17) Å, respectively. Despite the participation of the N1 atom in coordination to Zn, the C8—N1 bond length [1.311(3) Å] is close to the C1—N2 bond [1.304(3) Å]; the same applies to the second ligand with N4—C30 [1.310(3) Å] being experimentally close to the N5—C23 bond [1.309(3) Å]. The two five-membered chelate rings are planar [r.m.s. deviation = 0.028 Å (maximum deviation is 0.028 Å for the C1 atom) for the S1-chelate ring, and r.m.s. deviation = 0.058 Å maximum deviations are 0.043(1) and 0.043(2) Å for the S2 and N4 atoms of the S2-chelate ring, respectively]. The dihedral angle between the chelate rings is 78.53(6)° indicating a close to perpendicular relationship. The range of angles subtended at the Zn atom is a narrow 86.63(5)° for the N1—Zn—S1 chelate angle to a wide 129.24(5)° for N1—Zn—S2 chelate. These angles are consistent with a distorted tetrahedral geometry based on a N_2S_2 donor set. The distortion may be quantified buy the computation of τ_4 for a tetracoordinated geometry [10]. For (I), the value is 0.73 which matches most closely a regular tetrahedral geometry (τ_4 = 1.0) cf. a square-planar geometry (τ_4 = 0.0). Globally, the S1 and S2 atoms are cis-oriented in relation to the Zn atom.

Five closely related molecules are available in the literature for comparison. Three of them are N-phenyl derivatives with substituents in the 4-position of the terminal phenyl group connected to the ethylene residue, namely the 4-cyano and 4-chloro species [11] along with the 4-nitro derivative [12]; the 4-chloro species was characterised as a 1:1 THF solvate [11]. These molecules present, to a first approximation, very similar geometric characteristics as described above for (I) and indeed as observed for the two N-bound ethyl species with 4–H [13] and 4-methoxy [14] substituents. According to a recent systematic geometric analysis [12], the values of τ_4 in these complexes range from 0.70 to 0.74.

In the crystal of (I), several directional interactions have been identified with the aid of PLATON [15]. One of the amino–N—H atoms forms a hydrogen bond with a thiolato–S atom over a centre of inversion to form a dimeric synthon [N3—H3···S1^i: H3···S1^i = 2.62(2) Å, N3···S1^i = 3.4761(19) Å with angle at H3 = 168(2)° symmetry operation (i) $-x, 1-y, 2-z$]; there is no apparent, directional role for the N6—H6 group in the crystal packing. One of the non-coordinating imine–N atoms engages in an interaction with an aminophenyl–H atom [C26—H26···N5^{ii}: H26···N5^{ii} = 2.58 Å, C26···N5^{ii} = 3.517(3) Å with angle at H26 = 170° for (ii) $x, 3/2-y, -1/2+z$]. These interactions serve to link the dimeric agregates along the 2_1 screw axis. There are phenyl–C—H···π (phenyl) interactions between centrosymmetrically related chains [C34—H34···Cg(C9—C14)^{iii} = 2.72 Å with angle at H34 = 169° and C35—H35···Cg(C39—C44)^{iv} = 2.88 with angle at H35 = 137° for (iii) $1-x, 1-y, 1-z$ and (iv) $1-x, 1-y, 2-z$] within jagged supramolecular layers that stack parallel to (2 0 1). Given the absence of directional interactions between the layers, it was thought of interest to complement the above analysis with a study of the calculated Hirshfeld surfaces and of the full and delineated two-dimensional fingerprint plots using Crystal Explorer 21 [16] and published procedures [17].

The analysis showed that the Hirshfeld surfaces are mainly dominated by H···H contacts which comprise 54.5 % of the all contact surfaces with the tip of the decomposed fingerprint plot delineating to a H19···H36 interaction with a $d_i + d_e$ contact distance of 2.14 Å which is slightly shorter than the sum of van der Waals radii (ΣvdW) of 2.18 Å. The second most dominant contacts are attributed to H···C/C···H [27.6 %] with the pair of symmetric tips in the decomposed fingerprint plot arising from H35···C41/C41···H35 contacts with $d_i + d_e$ of 2.63 Å compared to the ΣvdW of 2.79 Å. The H···S/

S···H and H···N/N···H are the next most significant contacts with the respective contributions being 8.2 and 4.2 %. Both contacts exhibit a pair of pincer-like profiles in the decomposed fingerprint plots with the tips delineating to the reciprocal H3N···S1 and H26···N5 contacts with $d_i + d_e$ of 2.48 and 2.45 Å in contrast to the ΣvdW of 2.89 and 2.64 Å, respectively. The C···S/S···C contacts make a minor contribution to the Hirshfeld surface with the distribution being 2.6 % but with a meaningful $d_i + d_e$ of 3.43 Å, i.e. shorter than the ΣvdW of 3.50 Å.

Acknowledgments: The X-ray intensity data were collected by Dr M. I. M. Tahir, Universiti Putra Malaysia.
Author contributions: All the authors have accepted responsibility for the entire content of this submitted manuscript and approved submission.
Competing interests: The authors declare no conflicts of interest regarding this article.
Research funding: The synthetic aspects of this research was supported by the TARUC Internal Research Grant (Reference No.: UC/I/G201700023).

References

1. Agilent. CrysAlis^{PRO}; Agilent Technologies: Yarnton, UK, 2012.
2. Sheldrick G. M. A short history of *SHELX*. *Acta Crystallogr.* 2008, *A64*, 112–122.
3. Sheldrick G. M. Crystal structure refinement with SHELXL. *Acta Crystallogr.* 2015, *C71*, 3–8.
4. Farrugia L. J. WINGX and ORTEP for Windows: an update. *J. Appl. Crystallogr.* 2012, *45*, 849–854.
5. Parrilha G. L., dos Santos R. G., Beraldo H. Applications of radiocomplexes with thiosemicarbazones and bis(thiosemicarbazones) in diagnostic and therapeutic nuclear medicine. *Coord. Chem. Rev.* 2022, *458*, 214418.
6. Gupta S., Singh N., Khan T., Joshi S. Thiosemicarbazone derivatives of transition metals as multi-target drugs: a review. *Results Chem.* 2022, *4*, 100459.
7. Kostas I. D., Steele B. R. Thiosemicarbazone complexes of transition metals as catalysts for cross-coupling reactions. *Catalysts* 2020, *10*, 1107.
8. Tan M. Y., Kwong H. C., Crouse K. A., Ravoof T. B. S. A., Tiekink E. R. T. Crystal structure of 3-methyl-1-[(*E*)-(4-phenylbutan-2-ylidene)amino] thiourea, $C_{12}H_{17}N_3S$. *Z. Kristallogr. N. Cryst. Struct.* 2020, *235*, 1503–1505.
9. Tan M. Y., Kwong H. C., Crouse K. A., Ravoof T. B. S. A., Tiekink E. R. T. Crystal structure of bis{*N*-methyl-*N*′-[3-(4-methoxyphenyl)-1-methylpropane-1-ylidene]carbamohydrazonothioato}zinc(II), $C_{26}H_{36}N_6O_2S_2Zn$. *Z. Kristallogr. N. Cryst. Struct.* 2020, *235*, 1539–1541.
10. Yang L., Powell D. R., Houser R. P. Structural variation in copper(I) complexes with pyridylmethylamide ligands: structural analysis with a new four-coordinate geometry index, τ_4. *Dalton Trans*. 2007, 955–964. https://doi.org/10.1039/B617136B.
11. Barbosa I. R., Pinheiro I. D. S., dos Santos A. D. L., Echevarria A., Goulart C. M., Guedes G. P., da Costa N. A., de Oliveira e Silva B. M., Riger C. J., Neves A. P. Synthesis of copper(II) and zinc(II) complexes with chalcone-thiosemicarbazone hybrid ligands: X-ray crystallography, spectroscopy and yeast activity. *Transition Met. Chem.* 2018, *43*, 739–751.
12. Tan M. Y., Kwong H. C., Crouse K. A., Ravoof T. B. S. A., Tiekink E. R. T. Bis({*N*′-[3-(4-nitrophenyl)-1-phenylprop-2-en-1-ylidene]-*N*-phenylcarbamimidothioato}zinc(II): crystal structure, Hirshfeld surface analysis and computational study. *Acta Crystallogr*. 2021, *E77*, 839–846.
13. Tan M. Y., Crouse K. A., Ravoof T. B. S. A., Jotani M. M., Tiekink E. R. T. Bis(*N*′-{(*E*)-[(2*E*)-1,3-diphenylprop-2-en-1-ylidene]amino}-*N*-ethylcarbamimidothioato-κ^2N',*S*) zinc(II): crystal structure and Hirshfeld surface analysis. *Acta Crystallogr*. 2017, *E73*, 1001–1008.
14. Tan M. Y., Crouse K. A., Ravoof T. B. S. A., Jotani M. M., Tiekink E. R. T. Bis(4-methoxychalcone 4-ethylthiosemicarbazonato-κ^2N',*S*)zinc(II): crystal structure and Hirshfeld surface analysis. *Acta Crystallogr*. 2018, *E74*, 151–157.
15. Spek A. L. *checkCIF* validation ALERTS: what they mean and how to respond. *Acta Crystallogr*. 2020, *E76*, 1–11.
16. Spackman P. R., Turner M. J., McKinnon J. J., Wolff S. K., Grimwood D. J., Jayatilaka D., Spackman M. A. CrystalExplorer: a program for Hirshfeld surface analysis, visualization and quantitative analysis of molecular crystals. *J. Appl. Crystallogr.* 2021, *54*, 1006–1011.
17. Tan S. L., Jotani M. M., Tiekink E. R. T. Utilizing Hirshfeld surface calculations, non-covalent interaction (NCI) plots and the calculation of interaction energies in the analysis of molecular packing. *Acta Crystallogr*. 2019, *E75*, 308–318.